

From Lumps to Lattices: Crystallized Clots Made Simple

P. Ziherl^{*,†,‡} and Randall D. Kamien^{*,¶}

Faculty of Mathematics and Physics, University of Ljubljana, Jadranska 19, SI-1000 Ljubljana, Slovenia, Jožef Stefan Institute, Jamova 39, SI-1000 Ljubljana, Slovenia, and Department of Physics and Astronomy, University of Pennsylvania, 209 S. 33rd St., Philadelphia PA 19104-6396, USA

E-mail: primoz.ziherl@ijs.si; kamien@physics.upenn.edu

*To whom correspondence should be addressed

†Faculty of Mathematics and Physics, University of Ljubljana, Jadranska 19, SI-1000 Ljubljana, Slovenia

‡Jožef Stefan Institute, Jamova 39, SI-1000 Ljubljana, Slovenia

¶Department of Physics and Astronomy, University of Pennsylvania, 209 S. 33rd St., Philadelphia PA 19104-6396, USA

Abstract

Using a minimal model based on the continuum theory of a 2D hard-core/square-shoulder ensemble, we reinterpret the main features of cluster mesophases formed by colloids with soft shoulder-like repulsive interactions. We rederive the lattice spacing, the binding energy and the phase diagram. We also extend the clustering criterion [Likos, C. N., *et al.* Phys. Rev. E, **2001**, 63, 031206; Glaser, M. A., *et al.* EPL **2007**, 78, 46004] to include the effect of the hard cores, which precludes the formation of clusters at small densities.

Introduction

Generically, neutral colloidal particles attract each other via van der Waals and Casimir forces, and measures must be taken to prevent aggregation of clusters in both experimental systems and technological applications. One might be led to conclude that purely attractive hard-core particles could only form close-packed lattices or glassy messes. But the phenomenon of aggregation in colloids is not restricted to particles that attract each other. Over the past two decades clustering in purely repulsive pair potentials has been explored in some detail to find that it is distinguished by emerging order not seen in attractive particles. In particular, it has been established that at large enough density, clumping repulsive colloids can form superstructures with large voids on the order of many particle diameters.¹ Indeed, Malessio and Pellicane² demonstrated that even simple hard-core, square-shoulder potentials led to clustering purely on energetic grounds. The cluster morphologies and the clustering criterion itself have been studied theoretically using a range of approaches including liquid-state theory,³ lattice theory,^{4,5} density functional theory,⁶ and continuum models,^{5,7} and the predictions of the different approaches are remarkably consistent. Equally unequivocal are the results of numerical studies, mostly using Monte Carlo methods^{5,8} and direct search of minimal-energy configurations using genetic algorithms.^{9–11}

It is worthwhile at this juncture to step back and develop a minimal set of simple rules to expose the mechanism of lattice formation in these systems. It is our hope that these rules will make clear the essential ingredients needed for pattern formation in this large class of purely repellent

systems. Moreover, we develop these ideas in the context of real-space potentials and interactions yet recapitulate the clustering criterion of the more technical (though precise) Fourier-based analyses.^{1,3,5} Designing potentials in real space offers a more intuitive route to rational self-assembly and connects directly with, for instance, laser-trap and depletion based potentials.

In this note, we do this by using the continuum $T = 0$ model of the stripe phase formed by particles interacting via the hard-core/square-shoulder pair potential

$$U(r) = \begin{cases} \infty, & r < \sigma \\ \varepsilon, & \sigma < r < \lambda \\ 0, & r > \lambda \end{cases} \quad (1)$$

where σ and $\lambda > \sigma$ are the diameters of the core and the shoulder, respectively, and ε is the shoulder height.^{12,13} Characterized by a one-dimensional density modulation, the stripe phase is mathematically the most transparent of all cluster morphologies and our real-space analysis may be easier to visualize than reciprocal-space arguments.³⁻⁵ Moreover, by focusing on energy rather than on free energy we emphasize that the entropy does not promote clustering. These results are then extended to explore the generic phase diagram of the cluster-forming system at finite temperatures.

Clusters at $T = 0$

In the following, we first evaluate the energy of a two-dimensional hard-core/square-shoulder system with given hard-core diameter σ and shoulder diameter λ at a fixed average number density, and we minimize it with respect to intra-cluster density, cluster size, and lattice spacing. We consider the simplest cluster morphology, the one-dimensional square-wave of uniformly populated parallel stripes of width d and particle-free gaps of width $\ell - d$; the lattice spacing is ℓ . In the continuum model suitable in the large shoulder-to-core limit where λ is sufficiently larger than σ ,

the energy per particle can be related to the average overlap area per particle defined as

$$\omega = \frac{1}{2d} \int_0^d dy_1 \int d\mathbf{r}_2 \Theta(\lambda - |\mathbf{r}_2 - \mathbf{r}_1|), \quad (2)$$

where $\Theta(r)$ is the Heaviside step function describing the shape of the shoulder potential and \mathbf{r}_1 and \mathbf{r}_2 are the locations of particles 1 and 2, respectively, measured from the origin at an edge of the stripe in question. The first integration over y_1 , the distance of particle 1 from a stripe edge, is over the stripe containing particle 1 and the integration over \mathbf{r}_2 goes over all stripes. ω captures the interaction of the shoulders of particles, whereas the hard-core repulsion is treated in a mean-field approximation by demanding that the number density within stripes ρ_{stripes} be no larger than

$$\rho_{\text{cp}} = \frac{2}{\sqrt{3}\sigma^2} \quad (3)$$

corresponding to the close-packed hexagonal arrangement of the particles' hard-disk cores. This approximation is applicable in the broad shoulder regime $\lambda \gg \sigma$ and at densities large enough that the stripes are sufficiently wider than the core diameter so that speaking of ‘‘intra-cluster packing’’ of particles has meaning.

In terms of ω , the average energy per particle reads

$$E = \varepsilon \rho_{\text{stripes}} \omega. \quad (4)$$

But the number density of particles within stripes depends on their width relative to lattice spacing d/ℓ , which represents the fraction of the total area that is occupied by the stripes. In terms of the average density ρ ,

$$\rho_{\text{stripes}} = \frac{\rho \ell}{d}. \quad (5)$$

Since the energy is to be minimized at fixed ρ rather than at fixed ρ_{stripes} it is convenient to intro-

duce the scaled average overlap area

$$\Omega = \frac{\omega}{d/\ell} \quad (6)$$

which includes all dependence of

$$E = \varepsilon\rho\Omega \quad (7)$$

on d and ℓ . For the hard-core/square-shoulder pair interaction, Ω can be computed analytically but the result is too cumbersome to be of interest here.

We will now establish some rules of thumb.

I. Clusters are close-packed In [figure][1][1] we plot the reduced scaled average overlap area $\bar{\Omega} = \Omega/\lambda^2$ as a function of reduced lattice spacing $\bar{\ell} = \ell/\lambda$ for several stripe widths d/ℓ . The cluster-free, unmodulated phase corresponds to $\bar{\ell} = \bar{d} = 0$ and its nature depends on density: As argued below, its phase sequence includes the expanded fluid, the expanded hexagonal crystal, the condensed fluid, and the condensed hexagonal crystal. But since we treat the hard-core part of the pair interaction in a mean-field fashion, worrying only about the average number of neighbors within the reach of a particle's shoulder, the exact nature of the unmodulated phase is not crucial to understand why clustering takes place.

The uniform, unmodulated phase can be interpreted as a stripe morphology with a very fine density modulation such that the lattice spacing and the stripe width are much smaller than the two characteristic length scales of the pair potential, λ and σ . In this limit, $\bar{\Omega} = \pi/2$ irrespective of d/ℓ which tells us that for $d, \ell \ll \lambda$ the average energy per particle is $E = \pi\varepsilon\rho\lambda^2/2$. As $\bar{\ell}$ is increased, $\bar{\Omega}$ oscillates around $\pi/2$, reaches a global minimum at $\bar{\ell} \approx 1.2$, and then grows monotonically to saturate at a value of $\pi\ell/2d$. The large $\bar{\ell}$ behavior is a signature of macroscopic phase separation: At fixed d/ℓ , states with reduced lattice spacing $\bar{\ell}$ beyond ~ 1 correspond to thick stripe widths \bar{d} with an ever smaller number of particles residing at the boundary of the stripes. The average energy per particle is gradually dominated by that of the particles well within the bulk of the stripes, which reads $E = \pi\varepsilon\rho_{\text{stripes}}\lambda^2/2 = \pi\varepsilon\rho\lambda^2\ell/2d$ because the density within the stripes is larger than the average density by a factor of ℓ/d . This result gives $\bar{\Omega}(\ell \rightarrow \infty) = \pi\ell/2d$.

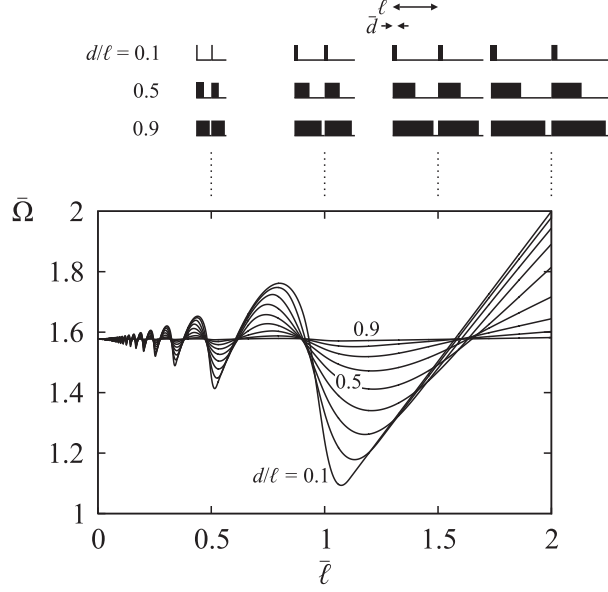


Figure 1: Reduced scaled average overlap area as a function of the reduced lattice constant $\bar{\ell} = \ell/\lambda$ for $d/\ell = 0.1(0.1)0.9$; for the sake of clarity, only curves corresponding to $d/\ell = 0.1, 0.5$, and 0.9 are labeled. The global minimum of the reduced scaled overlap area $\bar{\Omega}$ at $\bar{\ell} \approx 1.2$ is deepest for vanishingly small d/ℓ , which suggests that the equilibrium stripes are as compact as possible, *i.e.*, close-packed. The square density waves representing stripes with $d/\ell = 0.1, 0.5$, and 0.9 (top) schematically depict the stripe morphologies at $\bar{\ell} = 0.5, 1, 1.5$, and 2 ; the second column where $\bar{\ell} = 1$ corresponds to a lattice spacing exactly equal to the shoulder width.

The most important feature of this diagram is that the depth of the minimum decreases with increasing relative stripe width d/ℓ . This means that at any given average density $\rho = \rho_{\text{stripes}}d/\ell$, the system will select the state with the smallest possible d/ℓ at the expense of the density within stripes. For example, the curves corresponding to $d/\ell = 0.1$ and 0.2 represent two possible states of the system of a fixed average density ρ . According to [figure][1][1], the absolute minimum of the former is lower than that of the latter, which means that of the two stripe phases in question, the $d/\ell = 0.1$ state minimizes the total energy $E = \varepsilon\rho\lambda^2\bar{\Omega}$. But since the relative stripe width of the $d/\ell = 0.1$ state is half of that of the $d/\ell = 0.2$, the corresponding density within stripes must be twice as large as in the latter state. In other words, the ground state geometry of the stripes minimizes d/ℓ , restricted only by the close-packing limit forbidding stripes with $\rho_{\text{stripes}} = \rho\ell/d$ beyond the close-packed density ρ_{cp} . We conclude that at $T = 0$ the optimal stripes are made of

close-packed particles so that $\rho_{\text{stripes}} = \rho_{\text{cp}}$ and the reduced average number density

$$n = \frac{\rho}{\rho_{\text{cp}}} \quad (8)$$

coincides with d/ℓ .

II. Lattice spacing weakly depends on density An additional feature of the graphs in [figure][1][1] is that the equilibrium reduced lattice spacing, $\bar{\ell}_{\text{eq}}$, depends only weakly on d/ℓ . It is apparent that $\bar{\ell}_{\text{eq}}$ is largest at half-filling where it reaches 1.217, which nicely agrees with the value of 1.223 predicted by the lattice theory.⁵ It can be shown that the dependence of $\bar{\ell}_{\text{eq}}$ on n is well described by a parabola symmetric about $n = 0.5$. Even in the infinitely-dilute and close-packed limits, $\bar{\ell}_{\text{eq}}$ tends to 1 — but this result is of no physical consequence. As shown below, the binding energy vanishes in these two limits so that the clustering mechanism is not acting and the corresponding equilibrium reduced lattice spacings are irrelevant.

This observation is made even more compelling by employing observation I: Since the ground-state stripes are close-packed, we may as well switch back to the average overlap area per particle, ω and write the energy as $E = \varepsilon \rho_{\text{cp}} \omega$; $\bar{\omega} = \omega/\lambda^2$ can thus be regarded as the reduced energy. In [figure][2][2] we plot $\bar{\omega}$ as a function of reduced lattice spacing $\bar{\ell}$. It is apparent in this presentation that the location of the global minimum of $\bar{\omega}$ is little changed over the range $0.1 \leq n \leq 0.9$ and again we conclude that $\bar{\ell}_{\text{eq}}$ is roughly independent of n .

From [figure][2][2] we also extract the reduced binding energy $\Delta\bar{\omega}$ defined as the depth of the global minimum of $\bar{\omega}(n)$ at $\bar{\ell}_{\text{eq}}$ relative to the unmodulated phase at $\ell = 0$. The reduced binding energy shown in the inset to [figure][2][2] is a skewed U-shaped function of reduced average density which vanishes for $n = 0$ and $n = 1$. In an infinitely dilute system, the energy of the unmodulated phase itself tends to 0 and no spatial modulation of the density profile can reduce it further so that the binding energy is 0 too. On the other hand, a system of average density close to ρ_{cp} cannot undergo but a very restricted spatial modulation (because the density within the stripes should not exceed ρ_{cp}) and thus the energy gained upon clustering approaches 0 when $\rho \rightarrow \rho_{\text{cp}}$.

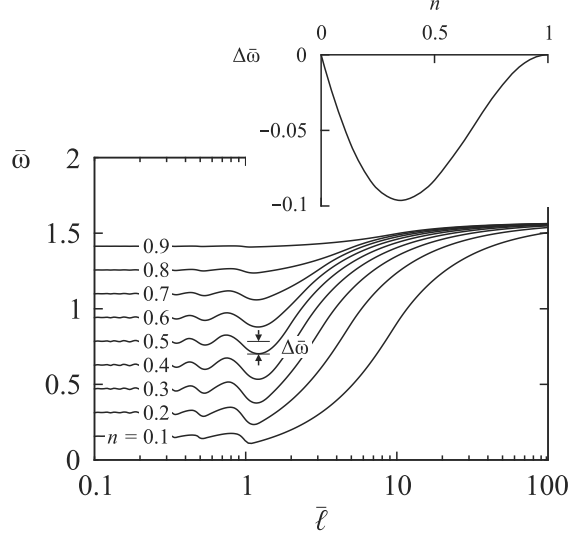


Figure 2: Reduced energy of the close-packed stripe morphology, $\bar{\omega}$, as a function of reduced lattice spacing $\bar{\ell}$ for $n = 0.1(0.1)0.9$. In the unmodulated phase at $\bar{\ell} = 0$, $\bar{\omega} = n\pi/2$. The inset shows the reduced binding energy $\Delta\bar{\omega} = \bar{\omega}(\bar{\ell}_{\text{eq}}) - \bar{\omega}(\bar{\ell} = 0)$ [as illustrated in the $\bar{\omega}(n = 0.5)$ curve] which is a skewed U-shaped function of reduced average density and vanishes at $n = 0$ and $n = 1$.

Although $\bar{\omega}$ and $\bar{\Omega}$ are closely related, they convey a somewhat different message. From [figure][1][1] we learned that the particles within the stripes are close-packed, which enabled us to directly relate the average density ρ to relative stripe width d/ℓ . On the other hand, [figure][2][2] exposes the binding energy of the equilibrium stripe morphology more clearly. But as far as the magnitude of the equilibrium lattice spacing is concerned, both quantities are equally telling.

Phase diagram

Our two observations can be used to qualitatively outline the phase diagram of the cluster phases in the temperature-density plane. To this end, we need to study the difference of the free energies of the stripe phase and the unmodulated phase, which consists of an energy term $\Delta E = \varepsilon\rho_{\text{cp}}\lambda^2\Delta\bar{\omega}$ and of an entropic term. The entropy of the two phases depends on their structure elaborated below in a semi-quantitative fashion.

At absolute zero, one of the hallmark features of the stripe morphology is its compact intra-stripe structure where the impenetrable hard cores of the particles are packed together as tightly

as possible at any reduced average density n . This state is materialized by the hexagonal lattice. Because of the robust, density-independent nature of this behavior, we posit that at finite temperatures the intra-stripe density ρ_{stripes} should not depend strongly on the reduced average density either (though it must be smaller than the close-packing density ρ_{cp}) and that the intra-stripe order remains hexagonal.

The structure of the unmodulated phases of hard-core/square-shoulder particles is more complicated and despite decades of efforts (see, e.g., Refs.^{15–17}), their thermodynamics remains only a partly solved problem. For the purpose of present discussion, it suffices to note that at low temperatures where they compete with cluster morphologies, the phase sequence of unmodulated phases consists of 4 variants, the 2 low-density and high-density phases being characterized with little and sizable overlap of particles' shoulders, respectively. At very small densities, the particles form an expanded fluid of disks of shoulder diameter λ (schematically shown in [figure][3][3]). As this fluid is compressed, it undergoes a transition to the expanded hexagonal crystal of disks of diameter λ . The location of the transition can be estimated by rescaling the phase diagram of the hard-disk system: $\rho_{\text{ef-ec}} \approx 0.792(\sigma/\lambda)^2\rho_{\text{cp}}$.²⁰ Upon further compression, the expanded hexagonal phase remelts to avoid close-packing; since the overlap of shoulders is increasingly less unfavorable at elevated temperatures, the phase transition density should decrease with temperature. From this transition on, the particles behave essentially as hard spheres of diameter σ and the transition to the condensed hexagonal phase takes place approximately at $\rho_{\text{cf-cc}} \approx 0.792\rho_{\text{cp}}$.²⁰

Understanding the main features of the sequence of unmodulated phases helps us to construct semi-qualitatively the entropic part of their free energy. We first note that the pressure of the hard-disk hexagonal crystal can be roughly regarded as a continuation of the hard-disk fluid branch²⁰ and we approximate the excess entropic free energy per particle in both the fluid and the crystal unmodulated phase by

$$F_{\text{ex}}^{\text{cond}}(n) = k_B T \left[\frac{\alpha n}{1 - \alpha n} - \ln(1 - \alpha n) \right] \quad (9)$$

where $\alpha = \pi/2\sqrt{3} \approx 0.907$. This prediction is based on the 2D Carnahan-Starling type theory for the fluid phase.^{21,22} Admittedly a rough approximation — it does not distinguish between the fluid

and the crystalline phase, and the hexatic phase is disregarded altogether — this excess entropic free energy provides a simple and adequate model across a broad range of reduced densities consistent with the scope of this analysis. Its main deficiency is the poor description of the crystalline phase (whose excess entropic free energy should diverge at reduced average density of $n = 1$ and not at $n = 1/\alpha = 1.103$). Yet we note that in the phase diagram of hard disks, the condensed crystalline phase is stable at $n > 0.792$ ²⁰ so that the discrepancy is limited only to large densities.

Using the model F_{ex} [Eq. (??)], we can outline the excess entropic free energy for the unmodulated phases. In [figure][3][3], we plot the excess free energy per particle of the expanded and the condensed phases, $F_{\text{ex}}^{\text{exp}}(n) = F_{\text{ex}}^{\text{cond}}((\lambda/\sigma)^2 n)$ and $F_{\text{ex}}^{\text{cond}}(n)$. The former diverges at $n = (\sigma/\lambda)^2/\alpha$ which corresponds to close-packed disks of diameter λ . This divergence is, of course, unphysical because the expanded hexagonal lattice remelts upon compression so that in this regime, the true excess entropic free energy interpolates between $F_{\text{ex}}^{\text{exp}}$ and $F_{\text{ex}}^{\text{cond}}$.

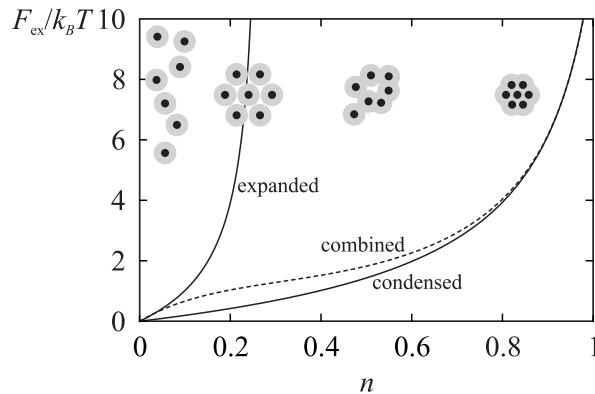


Figure 3: Excess entropic free energies per particle of the expanded and the condensed unmodulated phases derived using a Carnahan-Starling type theory (solid lines; the expanded phase corresponds to $\lambda/\sigma = 2$). The divergence of $F_{\text{ex}}^{\text{exp}}$ at $n = 0.276$ is unphysical; instead of approaching the shoulder-to-shoulder close-packed structure, the system melts to form the condensed fluid phase. The dashed line represents a qualitatively correct interpolation between the expanded and the condensed branch. — The schematics illustrate the structure of the 4 unmodulated phases: The expanded fluid, the expanded crystal, the condensed fluid, and the condensed crystal. Full circles indicate the hard cores of particles whereas the shaded coronas represent the shoulders.

The exact shape of the interpolating F_{ex} is not known. But our mean-field model is designed to work best for broad shoulders and in this case, the existence of the expanded phases is restricted to reduced average densities below $(\sigma/\lambda)^2/\alpha$, *i.e.*, to very small n . Being interested in the overall

behavior of the system, we may approximate the excess entropic free energy by the condensed branch alone. Then the total free energy difference can be constructed from overlap energy difference $\Delta E(n)$, the excess entropic free energy of the stripe morphology $F_{\text{ex}}^{\text{cond}}(n_{\text{stripes}})$, and the excess entropic free energy of the unmodulated phase $F_{\text{ex}}^{\text{cond}}(n)$:

$$\begin{aligned}\Delta F(n, n_{\text{stripes}}, \tau) &= \Delta E(n) + F_{\text{ex}}^{\text{cond}}(n_{\text{stripes}}) - F_{\text{ex}}^{\text{cond}}(n) \\ &= \varepsilon \rho_{\text{cp}} \lambda^2 \left\{ n_{\text{stripes}} \Delta \bar{\omega}(n) \right. \\ &\quad \left. + \tau \left[\frac{\alpha n_{\text{stripes}}}{1 - \alpha n_{\text{stripes}}} - \ln(1 - \alpha n_{\text{stripes}}) - \frac{\alpha n}{1 - \alpha n} + \ln(1 - \alpha n) \right] \right\} \quad (10)\end{aligned}$$

Here $n_{\text{stripes}} = \rho_{\text{stripes}}/\rho_{\text{cp}}$ is the reduced density within stripes, which should not depart much from 1 and must decrease with temperature, and

$$\tau = \frac{k_B T}{\varepsilon \rho_{\text{cp}} \lambda^2} \quad (11)$$

is the reduced temperature.

The clustering criterion The most important features of the total free energy difference are the negative skewed U-shaped energy term, whose exact dependence on the reduced average density shown in the inset to [figure][2][2] can be well fitted by

$$\Delta E \approx -0.65 \varepsilon \rho_{\text{cp}} \lambda^2 n(1-n)^2, \quad (12)$$

and the positive excess entropic free energy difference proportional to temperature which monotonically decreases from a finite value at $n = 0$ to 0 at $n = n_{\text{stripes}}$. We approximate the temperature dependence of the reduced density within stripes by a linearly decreasing function

$$n_{\text{stripes}}(\tau) = 1 - c\tau. \quad (13)$$

In the following, we choose $c = 6$: At the largest reduced temperature where the stripe morphology is stable, this gives $n_{\text{stripes}} \approx 0.9$ which is plausible.

In [figure][4][4]a, we plot ΔF for several values of reduced temperature τ . As τ is increased, the reduced average density range where the stripe morphology is stable gradually shrinks and at a large enough τ , the stripe morphology is disfavored at any n . Thus the phase diagram is characterized by a dome-like region of stability of the stripe morphology shown in [figure][4][4]b. Except at very large n where the differences between the unmodulated and the stripe phase are increasingly smaller and our model is inaccurate, the shape of the phase boundary reproduces well the clustering criterion obtained in terms of the lattice theory⁵ which states that instability occurs when

$$\frac{n(1-n)}{\tau} > \text{const.} > 0. \quad (14)$$

The agreement is indeed remarkable although our phase diagram lacks the symmetry about the half-filling point $n = 1/2$ encoded in Eq. (??). Needless to say, the model can be refined by better estimating the entropic part of the excess free energy.

Extending the clustering criterion The stripe morphology is subject to two consistency constraints. Firstly, adjacent stripes separated by more than a shoulder width do not interact with each other because there is no overlap of particles residing within them; without a restoring interstripe repulsion, such configurations would spontaneously disintegrate into thinner stripes with narrower gaps between them. This means that in the mechanically stable stripe state, the width of the particle-free gaps between stripes $\ell - d$ should be smaller than the shoulder diameter λ . A close inspection of [figure][1][1] shows that the global minimum at reduced lattice spacing $\bar{\ell} \approx 1$ is not compromised by this condition at any reduced average density n . Secondly, the stripe width must be larger than the hard-core diameter of the particles, $d > \sigma$; if not, speaking of close-packed stripes does not make sense. These two conditions bracket the physically relevant range of lattice spacing ℓ from top and from bottom, respectively. To compare the two bounds, we replace d by $n\ell$ so that i) the upper bound $\ell - d < \lambda$ becomes $\ell(1-n) < \lambda$ wherefrom $\ell < \lambda/(1-n)$ and ii) the

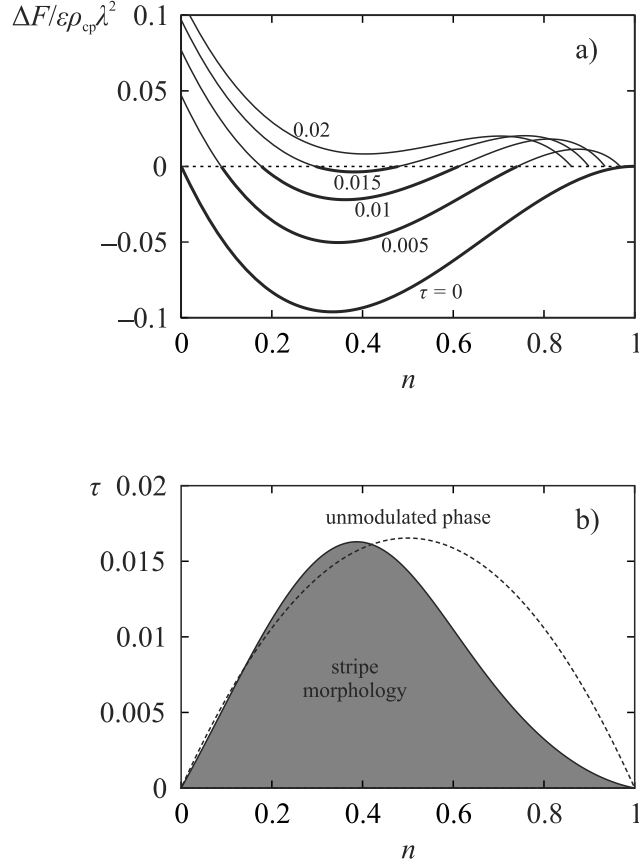


Figure 4: Free energy difference of the stripe and the unmodulated phase for n_{stripes} described by Eq. (??) and reduced temperature $\tau = 0, 0.005, 0.01, 0.015$, and 0.02 (panel a). As temperature is increased, the range of reduced average densities n where $\Delta F < 0$ and the stripe morphology is stable (thick sections of curves) becomes increasingly more narrow. Each curve terminates at $n^* \lesssim n_{\text{stripes}}(\tau)$ such that $\Delta F(n > n^*) < 0$; states beyond this point correspond to average density very similar to the density within stripes where the predictions of our model are meaningless. — Panel b) shows the temperature-density phase diagram of the hard-core/soft-shoulder stripe morphology and the unmodulated phase computed using the mean-field continuum model with the model $n_{\text{stripes}}(\tau)$ [Eq. (??)]. The stripe morphology is stable in the shaded region whose shape agrees rather well with the clustering criterion [dashed line; *const.* in Eq. (??) adjusted to reproduce the slope of the phase boundary at small reduced average densities].

lower bound $d > \sigma$ becomes $n\ell > \sigma$ and thus $\ell > \sigma/n$. We thus find that a stable phase can only exist if

$$n > \frac{\sigma}{\lambda + \sigma}, \quad (15)$$

the lower limit of stability of the stripe morphology. In view of the nature of the continuum model used here, this treatment of the hard-core part of the pair potential is expected to be valid for core-to-shoulder ratios λ/σ sufficiently smaller than 1.

Thus the effect of the hard-core part of the pair potential is to disfavor clustering at small densities, thereby restricting the validity of the criterion [Eq. (??)] to densities beyond a threshold determined by the core-to-shoulder ratio. Since the hard-core interaction is athermal, this condition should apply at all T as depicted in [figure][5][5].

Conclusions

The complete phase diagram will include the fluid and one or more crystal lattices as the low- and the high-density variants of the unmodulated, non-cluster phase. On top of the stripe morphology, in two dimensions there also exist the disk and the inverted disk cluster phase.⁵ Just like stripes are most stable at about $n = 0.4$ ([figure][4][4]) which corresponds to $\bar{\ell} \approx 1.2$ and $\bar{d} = 0.48$, the disks are expected to be bound most tightly at a similar lattice spacing and disk diameter. This configuration of disks will cover a smaller fraction of the plane and the corresponding average density will be smaller than 0.4. If we assume that the disks are stable in a dome-like region of the phase diagram qualitatively similar to that describing the stripes, the disk dome must peak at a density smaller than that of the stripe dome. Conversely, the inverted disk morphology should prevail at densities larger than 0.4. Moreover, the disk and the stripe phases occur in both the liquid and the solid intra-cluster order⁵ and so the generic full phase diagram of a cluster-forming ensemble should have a multiple-dome structure curbed by the fluid phase at small densities and by the crystal phases at large densities ([figure][5][5]). At large temperatures, the fluid-crystal phase transition line must be vertical because for $T \rightarrow \infty$, the system reduces to hard disks of diameter σ

which freeze and melt at $\rho/\rho_{cp} = 0.779$ and 0.792 , respectively.²⁰

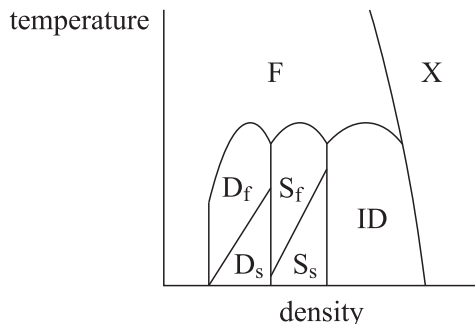


Figure 5: Generic phase diagram of cluster-forming repelling particles. At low temperatures, the phase sequence includes the fluid phase (F), several cluster morphologies (fluid disks — D_f , solid disks — D_s , fluid stripes — S_f , solid stripes — S_s , and inverted disks — ID), and one or more crystal phases (X). The vertical boundary of the disk morphologies at small densities indicates the restriction imposed by the hard-core part of the pair potential [Eq. (??)]. Regions of phase coexistence are not shown for clarity.

[figure][5][5] reproduces many features of the phase diagram obtained using a more complete treatment of the thermodynamics of a hard-core/square-shoulder system⁵ and it bears some similarity to the phase diagram of the hard-core/linear-ramp system.¹⁹ Although the width of the ramp studied in Ref.¹⁹ is too narrow for fully developed cluster phases, the non-close-packed lattices occurring in the phase diagram are very reminiscent of the cluster morphologies discussed here, and the phase diagram itself has roughly the same multidome shape as that in [figure][5][5]. We expect that for the hard-core/square-shoulder potential with small core-to-shoulder ratio, the agreement of the numerically obtained phase diagram with our prediction should be even better.

The ideas presented here capture the main mechanisms of cluster formation in systems of classical repelling particles in a way marked by the appeal of real-space description and by the analysis of the density-modulated morphologies across the whole range of lattice spacing. Given the seemingly counterintuitive behavior of particles with shoulder-type pair interaction, we hope that our rederivation will clarify the details of the more elaborate studies.

Acknowledgment

We thank H. Diamant, M. A. Glaser, G. M. Grason, C. J. Olson Reichhardt, C. Reichhardt, and C. D. Santangelo for helpful discussions and we acknowledge the hospitality of the Aspen Center for Physics where a part of this work was done. This work was supported by the Marie-Curie Initial Training Network COMPLOIDS under FP7-PEOPLE-ITN-2008 Grant No. 234810. PZ was supported by Slovenian Research Agency through Grant No. P1-0055. RDK was supported through NSF Grant DMR05-47230.

References

- (1) Klein, W.; Gould, H.; Ramos, R. A.; Clejan, I.; Mel'cuk, A. I. *Physica A* **1994**, *205*, 738-746.
- (2) Malescio, G.; Pellicane, G. *Nat. Mater.* **2003**, *2*, 97-100.
- (3) Likos, C. N.; Lang, A.; Watzlawek, M.; Löwen, H. *Phys. Rev. E* **2001**, *63*, 031206.
- (4) Shin, H.; Grason, G. M.; Santangelo, C. D. *Soft Matter* **2009**, *5*, 3629-3638.
- (5) Glaser, M. A.; Grason, G. M.; Kamien, R. D.; Košmrlj, A.; Santangelo, C. D.; Ziherl, P. *EPL* **2007**, *78*, 46004.
- (6) Likos, C. N.; Mladek, B. M.; Gottwald, D.; Kahl, G. J. *Chem. Phys.* **2007**, *126*, 224502.
- (7) Košmrlj, A.; Pauschenwein, G. J.; Kahl, G.; Ziherl, P. to be published.
- (8) Mladek, B. M.; Gottwald, D.; Kahl, G.; Neumann, M.; Likos, C. N. *Phys. Rev. Lett.* **2006**, *96*, 045701.
- (9) Fornleitner, J.; Kahl, G. *EPL* **2008**, *82*, 18001.
- (10) Pauschenwein, G. J.; Kahl, G. *Soft Matter* **2008**, *4*, 1396-1399.
- (11) Pauschenwein, G. J.; Kahl, G. J. *Chem. Phys.* **2008**, *129*, 174107.

- (12) Kincaid, J. M.; Stell, G.; Goldmark, E. J. *Chem. Phys.* **1976**, *65*, 2172-2179.
- (13) Young, D. A.; Alder, B. J. *Phys. Rev. Lett.* **1977**, *38*, 1213-1216.
- (14) Kirkwood, J. G. *J. Chem Phys.* **1950**, *18*, 380-382.
- (15) Rascón, C.; Velasco, E.; Mederos, L.; Navascués, G. J. *Phys. Chem.* **1997**, *106*, 6689-6697.
- (16) Lang, A.; Kahl, G.; Likos, C. N.; Löwen, H.; Watzlawek, M. J. *Phys. Condens. Mat.* **1999**, *11*, 10143-10161.
- (17) Singh, M.; Liu, H.; Kumar, S. K.; Ganguly, A.; Chakravarty, C. J. *Chem. Phys.* **2010**, *132*, 074503.
- (18) Carnahan, N. F.; Starling, K. E. *J. Chem. Phys.* **1967**, *51*, 635-636.
- (19) Jagla, E. A. *Phys. Rev. E* **1998**, *58*, 1478-1486.
- (20) Binder, K.; Sengupta, S.; Nielaba, P. J. *Phys. Condens. Mat.* **2002**, *14*, 2323-2333.
- (21) Maeso, M. J.; Solana, J. R. *J. Chem. Phys.* **1993**, *99*, 548-552.
- (22) Hansen, J.-P.; McDonald, I. R. *Theory of Simple Liquids* (Academic Press, London, 1986).

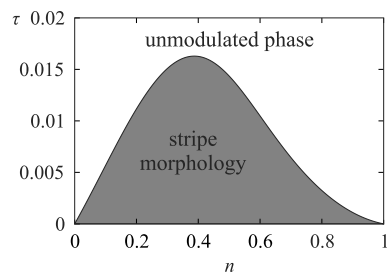


Figure 6: Ziherl and Kamien: Graphic for the Table of contents